Evaluation of Bone Regeneration Using the Rat Critical Size Calvarial Defect

Patrick P. Spicer[1,#], **James D. Kretlow**[1,2,#], **Simon Young**[3], **John A. Jansen**[4], **F. Kurtis Kasper**[1], and **Antonios G. Mikos**[1,*]

[1]Department of Bioengineering, Rice University, Houston, TX, USA [2]Department of General Surgery, Division of Plastic Surgery, Baylor College of Medicine, Houston, TX, USA [3]Department of Oral and Maxillofacial Surgery, The University of Texas at Houston Health Science Center, Houston, TX, USA [4]Department of Biomaterials, Radboud University Nijmegen Medical Centre, Nijmegen, The Netherlands

Abstract

Animal models that are reliably reproducible, appropriate analogues to the clinical condition they are used to investigate, and that offer minimal morbidity and periprocedural mortality to the subject are the keystone to the preclinical development of translational technologies. For bone tissue engineering, a number of small animal models exist. Here we describe the protocol for one such model, the rat calvarial defect. This versatile model allows for evaluation of biomaterials and bone tissue engineering approaches within a reproducible, nonload-bearing orthotopic site. Critical steps to ensure appropriate experimental control and troubleshooting tips learned through extensive experience with this model are provided. The surgical procedure itself takes approximately 30 minutes to complete with approximately 2 hours of perioperative care, and tissue harvest is generally performed 4 to 12 weeks postoperatively. Several analytical techniques are presented, which evaluate the cellular and extracellular matrix components, functionality and mineralization, including histological, mechanical and radiographic methods.

Keywords

tissue engineering; animal model; bone regeneration; regenerative medicine; biomaterials

INTRODUCTION

Bone regeneration represents a significant component of clinical practice aimed at filling defects arising from trauma, congenital defects and tumor excision. While numerous current clinical strategies can be applied to address these defects, the non-union defect [See Box 1], defined as incomplete closure of the defect, remains a clinical challenge.[1,2] Many different

strategies are currently being investigated to address the challenge presented by non-union; however, adequate testing of such strategies is necessary before they can be translated into human use. Historically and at present, animal testing of pharmaceuticals, medical devices, and medical strategies has played a key role in the translation of many therapeutics into the clinic. Despite ethical concerns and efforts to develop alternatives to animal experimentation, a critical component in translational sciences and medical technology development are standardized animal models.

Box 1

Definition of a critical size defect

In the case of bone, an orthotopic defect that will not heal without intervention is termed a "critical size defect." By classical definition, a critical size defect is the smallest size tissue defect that will not completely heal over the natural lifetime of an animal.[3,16] Current use of the term, which some researchers argue should be abandoned,[22] deviates slightly from this definition in that many accepted models have not undergone the testing necessary to ensure that they meet the criteria of being smallest in size. Additionally, most are evaluated at an experimental endpoint rather than the end of the natural lifetime of the subject. While the term "nonhealing" may be more appropriate, for consistency, models generally referred to as "critical size" in the literature will be called so here. As such, materials or strategies, which cause complete regeneration of the bone in these defects, are considered to bridge non-union defects, or capable of generating bone at a site and time when bone would otherwise not be present. However, these critical size defects should be contrasted with defects in which a pathological process, and not size, results in non-union.[8]

Animal Models for Bone Regeneration

In bone tissue engineering and osteoinductive biomaterial development, a number of animal models are available.[3–7] In our experience within these fields, the ideal animal model has the following characteristics: is highly reproducible, can be used for the assessment of multiple types of materials or strategies, is relevant to a clinical situation of interest, allows for multiple types of analysis, and offers little morbidity and mortality to the animal prior to the planned experimental endpoint. Other practical factors to consider when evaluating animal models are the time required to generate data with appropriate statistical power, the associated costs, and the learning curve required for competency in performing the necessary experimental steps. Finally, in theory, orthotopic animal models allow the most clinically relevant assessment of a biomaterial or strategy for non-union applications.[8]

Many species have been used for animal models of bone defects, including mice, rats, rabbits, dogs, pigs, sheep and goats, but much of the research has focused on rodent models due to reproducibility, through-put and economic considerations.[3–7] Anatomically, many areas of the rodent skeleton can serve as recipient sites of orthotopic defects, including the femora, spine, mandible and calvarium.[3,9–14] First described in 1973 but not truly established until the work of Takagi and Urist 10 years later,[15,16] the rat calvarium allows for a reproducible defect that can be generated quickly and does not require fixation for stabilization of the skeleton, as is generally required with femoral defects. However, as an anatomical site experiencing less loading than long bones, the functional testing of a bone regeneration strategy intended to withstand biomechanical forces is not feasible in the calvarial defect. Additionally, the calvarial defect serves as a model for intramembranous bone formation and thus may be less applicable to biomaterials or strategies for endochondral bone formation. Finally, functional assessment of the bone regeneration *in*

vivo is not possible in the calvarial defect but can be done in other models.[17] Thus taking into consideration the objective of the biomaterial or bone regeneration strategy, the rat calvarial defect can serve as a rapid, high throughput method for *in vivo* evaluation of bone regeneration.

For the rat calvarial defect, 8 mm is generally accepted to be of critical size; however, smaller defects have been investigated in models with 2 defects per animal, allowing fewer animals to be required for a given study.[18] This advantage must be thoughtfully considered with respect to the objectives of a study, as a subcritical size defect can heal without intervention. Additionally, the potential for interactions between these two adjacent defects should be considered. Lastly, studies whose primary goal is the regeneration of bone in a defect where natural regenerative capacity no longer suffices should avoid such designs. The rat calvarial defect can be used to evaluate bone regeneration and screen different biomaterials or tissue engineering constructs before moving to larger animals for potential translation to human applications in the craniofacial complex.[19] This protocol describes the preparation, surgical technique and possible analyses of bone regeneration in the rat calvarial defect, which has been used for over the last decade in our laboratory.

Overview of the evaluation of bone regeneration in the rat calvarial defect

The creation of the calvarial defect is accomplished primarily by the use of a dental trephine with a dental drill against the superficial aspect of the calvarium. This exposure is achieved through midline incision and spreading of the skin, fascial and periosteal layers overlying the sagittal suture of the calvarium. The bone is not completely penetrated by the trephine to avoid damage to the underlying dural and brain tissues as the dura may play a role in bone healing and regeneration.[20–22] Instead the bone is thinned considerably and elevated using blunt instruments to separate the bone from the underlying dura. Once the bone is excised, the biomaterial or bone regeneration strategy can be implanted and the wound closed by suturing the periosteal and skin layers. Experimental controls are a critical aspect of the study design and typically include an empty defect and a clinical standard of bone regeneration, such as autograft, as negative and positive controls, respectively.[23–27]

Several analysis methods are available for evaluating bone regeneration in the rat calvarial defect. In addition to histological techniques to visualize the tissue present in the defect, more structural and functional assessments are possible through radiographic and mechanical analysis. Push-out testing can assess the interfacial strength of the tissue bridging the gap between the native bone and the bone regenerative technology in the defect. Such functional assessment is critical for bone regeneration evaluation as the mechanical properties of regenerated bone are a critical requirement to its function. Also, as the defect is relatively 2-dimensional, planar radiography can assess the bridging of the defect by mineralized tissue. Advances in radiographic analysis, such as microcomputed tomography (microCT) allow for the 3-dimensional reconstruction of mineralized tissue within the defect, visualizing the volumetric and spatial density of bone regeneration of the tissue. Additionally, with radiopaque curing solutions, such as MicrofilR, assessment of angiogenesis, an important precursor to osteogenesis,[24] in the defect is also possible. In addition to standard histological techniques, the use of fluorochromes, fluorescent molecules that are incorporated into remodeling or forming bone, can temporally label bone growth for visualization after histological sectioning.

The reproducibility of the model can be assessed by comparing controls across experiments. Empty defects, commonly used as a negative control have been shown to result in 5–15% of the volume of the defect filled with mineralized matrix as measured by microcomputed tomography.[24,28] Additionally, the empty defect has consistently shown to result in a thin fibrous tissue within the defect with no visible bone regeneration.[16,24,29,30]

Several strains have been utilized for rat calvarial defects including Fisher 344, Sprague-Dawley and Wistar rats.[16,23–25,29–33] Strain selection should be determined weighing experimental needs such as inbred strains for syngeneic cell transplantation against economic constraints. Our laboratory has worked primarily with Fisher 344 rats as they are inbred and allow for the transplantation of cells from one rat to another.

MATERIALS

Reagents

- Implant material including appropriate control material, if applicable

- Buprenorphine (Henry Schein, catalog number 1217793)

- Isoflurane (Henry Schein, catalog number 1084262)

   Caution: Isoflurane is a United States Food and Drug Administration Pregnancy Class C drug. Pregnant individuals should avoid exposure to the drug. For safety purposes, a scavenging system should be employed if possible and isoflurane exposure badges can be worn to measure workers' cumulative exposure during the course of experiments.

- Lidocaine, 1 wt/vol% with 1:100,000 epinephrine (Henry Schein, catalog number 1047099)

- Sterile normal saline (Henry Schein, catalog number 6985812)

- Formalin (Fisher Scientific, catalog number SF100)

- Skeletally mature rats (We use inbred Fisher 344 rats, 11–12 week old, male, Harlan, catalog number F344/NHsd; however, inbred Lewis[34] and outbred Sprague-Dawley[28,30,35] and Wistar[25] rats have been used.)

   Caution: All animal experiments require approval by the appropriate institutional animal care and use committees and must be conducted in accordance with institutional, local, national, and funding agency guidelines and regulations. Rats must be skeletally mature as weanling rats have shown spontaneous regeneration of critical size defects.[16]

- Heparin (Henry Schein, catalog number 1162402)

- MicrofilR and curing agent (Flow Tech Inc., catalog number MV-122)

- Diluent (Flow Tech Inc., catalog number MV-Diluent)

- Alizarin-complexone (Sigma, catalog number 122777)

- Calcein (Sigma, catalog number C0875)

- Phosphate buffered saline (Gibco, catalog number 21600010)

- Ethanol, 70% (VWR, catalog number 71001-654)

- Oxygen, USP Grade (Matheson Tri-Gas)

- Carbon dioxide, USP Grade (Matheson Tri-Gas)

Equipment

- Electric clippers (Oster, Model A2)

- Scale (Pelouze, Model PE5)

- Lacrilube (Henry Schein, catalog number 3773656)

- Rodent Anesthesia System (VetEquip, Table Top System)

- Rodent heart rate monitor and pulse oximeter (Nonin Medical)

- Alcohol swabs (Covidien, catalog number 5110)

- Iodine swabsticks (Dynarex, catalog number 1201)

- Sterile, disposable scalpel blade, #15 (Miltex, catalog number 4-115)

- Scalpel handle (KLS Martin, catalog number 10-130-03 or 10-130-05)

- Surgical/dental drill (NSK Surgic XT Plus, catalog number Y141246)

- Contraangle handpiece (NSK Ti-Max, catalog number SG20L)

- Straight handpiece (NSK Ti-Max, catalog number SG65L)

- Small needle driver (KLS Martin, catalog number 20-634-13)

- Small self retaining retractor (KLS Martin, catalog number 15-723-10 or 15-701-05)

- Adson-Brown forceps (KLS Martin, catalog number 12-244-12)

- Small hemostat (KLS Martin, catalog number 13-310-12)

- Elevator (Hu-Friedy catalog number PFITR)

- 8 mm diameter trephine (Ace Surgical, catalog number 04-9487-01)

- 1 mm cross-cut bur (Stryker Leibinger, catalog number 277-10-210)

- 18 gauge needle (Becton Dickinson, catalog number 305195)

- 25 gauge needle (Becton Dickinson, catalog number 305122)

- 27 gauge needle (Becton Dickinson, catalog number 305109)

- 1 mL syringe (Becton Dickinson, catalog number 309659)

- 5 mL syringe (Becton Dickinson, catalog number 309603)

- Syringe filter (Thermo Scientific, catalog number 192-2520)

- Personal protective equipment: eye protection, sterile gown, sterile gloves, surgical cap and mask (VWR, catalog number 89187-986; Cardinal Health, catalog numbers 9515 and 2D7254; Medline Industries Inc., catalog number NON28625; Kimberly Clark Healthcare, catalog number 48201)

- Sterile gauze (Henry Schein, catalog number 1002524)

- 4-0 Monocryl Monofilament RB-1 (Ethicon, catalog number Y304H)

- 3-0 Plain Gut Monofilament FS-2 (Ethicon, catalog number H822H)

- Light microscope with fluorescent filters (Zeiss AxioImager.Z1 with AxioCam MRc 5 and Alexa Fluor 4568 (AF4568, alizarin) and AF488 (calcein))

- Cabinet planar radiography system (Faxitron 43855A)

- Compressive mechanical testing system (MTS 858 Mini Bionix II testing system)

- Push-out testing jig (Custom made part fabricated per specifications from previous studies[23,36] and shown in Figure 1a)

- Low force load cell (Transducer Techniques 100 lb load cell, catalog number MDB-100)

- Angiocatheter (Venisystems, Abbocath-T 18G catalog number 4535-08)

- Syringe pump (Cole-Parmer, catalog number 780100C)

PROCEDURE

Preoperative Preparation (Timing: should take approximately 20 minutes to complete excluding sterilization cycle and cooling)

1   Sterilize all surgical instruments in an autoclave and allow time to cool to room temperature (20–25°C). Sterilize the operating table/surface with copious amounts of 70% (vol/vol) ethanol.

2   Place the rat into the induction chamber and anesthetize using 4% isoflurane in oxygen for approximately 2 min.

3   After induction transfer the animal from the induction chamber and maintain anesthesia with 2% isoflurane delivered via nosecone/non-rebreather. Assess depth of anesthesia by lack of reflex to toe pinch. Weigh the rat. Using an 18 gauge needle for saline injection and a 25 gauge needle for buprenorphine and appropriately sized syringes, give intraperitoneal injections of 0.05 mg/kg buprenorphine for perioperative analgesia and 5 mL/kg sterile normal saline to account for fluid losses during surgery.

Caution: Administration of 5 mL/kg sterile normal saline assumes an operative time of approximately 30 minutes. In cases where the operative time differs, a preoperative dose of sterile normal saline should be given based on 10 mL/kg/hr of surgery.

4   Shave the rat from the bridge of the snout between the eyes to the caudal end of the skull/calvarium using electric clippers. After shaving, an alcohol swab can be used to remove hair trimmings. Apply Lacrilube to each eye.

5   Transfer the rat onto a heating pad set to 37°C on the operating field; maintain isoflurane at 2% in oxygen via nosecone/non-rebreather. Attach the pulse oximeter/heart rate monitor to the foot. Paint the shaved field and surrounding areas with the iodine swabs, taking care not to apply the solution over the eyes. Place a sterile drape over the body.

TROUBLESHOOTING

Critical Step: Monitor heart rate and oxygen saturation throughout the procedure to allow improved assessment of the depth of anesthesia.

6   Don personal protective equipment. Clean off iodine scrub using sterile saline and gauze. Inject 0.5 mL of 1% lidocaine with 1:100,000 epinephrine subcutaneously along the sagittal midline of the skull.

Operative Procedure (Timing: should take approximately 30 minutes to complete)

7   Using the scalpel, make an approximately 1.5 cm incision down to periosteum over the scalp from the nasal bone to just caudal to the middle sagittal crest or bregma. Apply countertraction laterally and visualize the calvarium as seen in Figure 2a. Sharply divide the periosteum covering the calvarium down the sagittal midline with the scalpel, and then gently push the periosteum laterally

while elevating from the underlying skull using the elevator as shown in Figure 2b.

TROUBLESHOOTING

Critical Step: An adequate incision and resultant surgical exposure is necessary to prevent soft tissue/periosteal injury during the trephination of the calvarial defect. Consistency is necessary as variable periosteal injury may alter bone growth among specimens, leading to confounding results.[37] When elevating the periosteum, lateral borders will be encountered beyond which the periosteum cannot be elevated. These define the limits of the surgical field/exposure.

8 Insert a self-retaining retractor or manually retract to spread the soft tissues and expose the underlying bone. Irrigate with sterile normal saline.

9 Score the calvarium with the surgical drill and trephine operating at 1500 rpm or less. Irrigate the trephine and calvarium with sterile normal saline dropwise at approximately 1 drop every 2 seconds. The slow speed of the trephine and irrigation are critical to prevent thermal injury, which can damage the tissue at the defect margins and produce confounding results.[38]

TROUBLESHOOTING

Critical Step: Care must be taken to score the calvarium without penetrating too deeply. Lateral to the sagittal midline, the calvarium slopes downward, so slight precession of the trephine is necessary to score the lateral portions of the defect margin without penetrating at the caudal and cranial defect margins, as the sagittal sinus lies deep to these portions of the defect. Furthermore, care must be taken not to damage the divided periosteum.

10 Continuing the trephination, apply at most gentle pressure while precessing the trephine around the scored defect margins as shown in Figure 2c.

Critical Step: The calvarium is approximately 1 mm thick. Markings on the trephine can serve as landmarks to indicate depth and should be monitored throughout the drilling process. To prevent dural or brain injury, the applied downward pressure should be less than the weight of the drilling handpiece. Throughout this process, the trephine can be withdrawn and the defect margins assessed as shown in Figure 2d. As the calvarium at the defect thins, it will become translucent so that the dura and cortex can be visualized. Assess the depth of the cut by gently applying pressure with the elevator around the inner portion of the defect margins. As the defect nears the appropriate thickness, the trephinated portion of bone will be able to be displaced downward with slight pressure, indicating a near full thickness cut through the calvarium.

11 As shown in Figure 3a, place the elevator blade into the defect margin and, moving circumferentially around the defect, apply gentle pressure to complete the defect by lifting gently with the elevator. Carefully slide the blade of the elevator under the freed calvarium and sweep back and forth, freeing the dura from the underside of the bone as seen in Figure 3b.

TROUBLESHOOTING

Critical Step: Free the lateral portions of the dura first, taking care when crossing the midline and completing the defect/freeing the dura at the cranial and caudal aspects as the dura forms the superficial boundary of the sagittal sinus. Dural injury overlying the sinus will lead to hemorrhage and has been shown to influence bone regeneration thus creating confounding results.[20,39–41]

12 Once the dura has been freed, use the elevator as a lever arm to raise the calvarium off the dura, finishing the defect as shown in Figure 3c. The periphery of the defect should be assessed for any remaining bone fragments. If present, the remaining fragments should be carefully removed using the elevator.

13 Wash the defect copiously with sterile normal saline to remove any debris and/ or bone chips. Place the implant material into the defect.

Critical Step: Care must be taken to avoid excessive pressure on the brain when implanting the material. Malleable or gel-like materials should be conformed to the defect site. This can be accomplished through *ex situ* or gentle *in situ* molding using the elevator.

14 Close the periosteum over the implant using a running 4-0 monocryl suture.

Critical Step: Without the intact calvarium, intracranial pressure will produce a mild bulge of the cortex through the defect, so most implants will initially sit on the dura rather than within the defect. The periosteum can be fragile/friable. Handle it gently using forceps and a tapered needle to avoid tears. Implants with thickness greater than 1.5 mm require closing the periosteum under increased tension, potentially predisposing it to tears or increasing pressure on the brain below. To aid in initiating closure of the periosteal layer, the 4-0 monocryl suture can be passed each side of the incised periosteum immediately after elevation (Step 7) as shown in Figure 3c, such that the suture can be gently pulled to bring the periosteum into apposition.

15 Close the skin over the periosteum using running or simple interrupted 3-0 plain gut suture.

Postoperative Care (Timing: should take approximately 1.5 hours to complete)

16 After completion of surgery, carefully clean the head with saline or dilute hydrogen peroxide to remove any blood. Turn the isoflurane off and monitor the rat on 100% oxygen by nosecone/non-rebreather. At signs of purposeful movement, transfer the rat to a warmed incubator with supplemental oxygen.

TROUBLESHOOTING

17 At the completion of observation, transfer rats to normal husbandry cages and house singly until tissue harvest. Give three postoperative doses of buprenorphine for analgesia at 8–12 h, 20–24 h, and 32–36 h.

TROUBLESHOOTING

Critical step: Avoid the use of nonsteroidal anti-inflammatory medications in the perioperative and postoperative period as these potentially affect bone healing and regeneration.[42,43]

Fluorochrome Labeling (Timing: 5 min per injection)

18 One week postoperatively prepare Alizarin-complexone solution. Dissolve Alizarin-complexone in isotonic sodium bicarbonate solution (150 mEq/L) at a concentration of 15 mg/mL and filter through a 0.2 μm sterile syringe filter.

CRITICAL STEP Fluorochrome solutions need to be prepared immediately prior to injection.

19 Weigh rat and inject Alizarin-complexone (25 mg/kg or 1.67 mL/kg of the prepared solution) subcutaneously to fluorescently label tissue undergoing bone

formation or remodeling red. Continue to house rats singly in normal husbandry cages.

20 Three weeks postoperatively, dissolve Calcein in isotonic sodium bicarbonate solution (150 mEq/L) at a concentration of 20 mg/mL and filter through a 0.2 μm sterile syringe filter.

21 Weigh rat and inject Calcein (25 mg/kg or 1.25 mL/kg of the prepared solution) subcutaneously to fluorescently label tissue undergoing bone formation or remodeling green. Continue to house rats singly in normal husbandry cages.

Euthanasia and Implant Harvest (Timing: should take approximately 0.5 hours to complete)

22 4 or 12 weeks postoperatively place the rat into the induction chamber and anesthetize using 4% isoflurane in oxygen.

23 After induction, stop the flow of oxygen into the induction chamber and asphyxiate using 2 L/min flow of carbon dioxide for 5 min or until breathing movements cease for 1 min.[44]

24 Perform a bilateral thoracotomy (option 24A) or thoracic dissection (option 24B). Perform a bilateral thoracotomy if the sample is for mechanical testing, histology, or radiography. Perform a thoracic dissection if the sample is for vascular assessment with microCT using MicrofilR.

CAUTION NIH guidelines purport "A secondary method of euthanasia (e.g., thoracotomy or exsanguination) can be also used to ensure death."[45]

    A. Bilateral thoracotomy

        i. Remove the rat from the induction chamber and perform a bilateral thoracotomy by piercing through the intercostal spaces of the ribs with a needle or scalpel on the right and left sides of the chest.

        ii. To retrieve the implant, incise between the medial canthi of the eyes down to the bone and another incision connecting the lateral canthi of the eyes over the parietal bones and occiput of the cranium.

        iii. Remove the overlying skin by blunt dissection, taking care not to disturb the implant.

        iv. Using a 701 cutting bur and a surgical drill, cut the cranium following the same lines used for the incision above between the medial canthi and connecting the lateral canthi circumferentially around the cranium.

        v. Remove a section of the cranium containing the implant.

    B. Thoracic Dissection

        i. Remove the rat from the induction chamber and clip the chest free of fur.

        ii. Using a scalpel, make an anterior midline incision from the forelimbs to the xyphoid process.

        iii. Using scissors, cut the ribs just left of the sternum and retract the ribs laterally, exposing the thoracic cavity.

iv. Using a hemostat, clamp the descending aorta completely closed and insert an angiocatheter into the left ventricle.

v. Using a scalpel, incise the inferior vena cava and immediately begin perfusing 20 mL of heparinized normal saline (100 U/mL) at 2 mL/min through the angiocatheter using a syringe pump.

vi. Following the saline solution, perfuse 20 mL of MicrofilR solution (4:5 ratio of MicrofilR:diluent with 5% curing agent) at 2 mL/min using a syringe pump.

vii. Allow the MicrofilR to cure overnight by storing the euthanized rat at 4°C.

Critical Step: Perfusion with MicrofilR and immunohistochemistry methods used together may require modifications to the above protocol to maintain protein structure for proper immunohistochemical staining.

viii. To retrieve the implant, incise between the medial canthi of the eyes down to the bone and another incision connecting the lateral canthi of the eyes over the parietal bones and occiput of the cranium.

ix. Using a 701 cutting bur, straight handpiece and a surgical drill, cut the cranium following the same lines used for the incision above between the medial canthi and connecting the lateral canthi circumferentially around the cranium at 40,000 rpm.

x. Remove a section of the cranium containing the implant.

Critical Step: The skin and brain should be left in contact with the section of cranium, which is removed, to maintain the integrity of any vessels through the implant region.

TROUBLESHOOTING

25 Place extracted tissue into 10% buffered formalin if proceeding with histological analysis (option 25A) or cold phosphate buffered saline (pH = 7.4) if proceeding with mechanical analysis (option 25B).

Caution: Formalin is an irritant to skin and eyes and a possible carcinogen. All work should be conducted in a chemical fume hood or well ventilated area to decrease exposure. Personal protective equipment, including a lab coat, gloves and safety glasses should be worn when using formalin.

Critical Step: Samples can be used for several analyses as several of the analytical techniques are non-destructive. Mechanical and histological analyses are the only destructive techniques described in this protocol and thus cannot be completed on the same samples. Radiography can be completed before either mechanical or histological analysis.

A. Histological Analysis

i. Make a reference mark, such as a notch, in the bone outside the defect area to ensure proper orientation in subsequent analysis.

ii. Place the extracted tissue into 50 mL of 10% buffered formalin for 72 hr at 20°C in a specimen container.

Critical Step: For immunohistochemistry staining, fixation should be kept to a minimum for best results.

iii. After 72 hr, place the extracted tissue into 70% ethanol in water.

PAUSEPOINT Samples can be stored at 20°C in 70% ethanol in water for at least 3 months.

iv. If radiographic analysis will be performed, then proceed to step 26; otherwise proceed to step 27A.

B. Mechanical Analysis

i. Place the extracted tissue into 50 mL of cold phosphate buffered saline (pH = 7.4) in a specimen container on ice.

ii. If radiographic analysis will be performed, then proceed to step 26; otherwise proceed with mechanical analysis (step 27B) within 1 hr of euthanasia.

Alternatively, samples for mechanical testing can be frozen in saline soaked gauze and tested once thawed.[46] PAUSEPOINT Samples can be frozen at 4°C in saline soaked gauze for at most 3 months.

Radiographic Analysis (Should take approximately 5 minutes for planar radiography and 2 hours for microCT)

26 Perform radiographic analysis with either planar radiography (option 26A) or microcomputed tomography (option 26B).

A. Planar Radiography

i. Remove the specimen from the 70% ethanol and place flat on the film cassette with the cerebral surface facing up.

ii. Expose the specimen for 10 s at 25 kVp and 3 mA.

Troubleshooting

iii. Score each planar radiograph. This may be done using the scoring system described in Figure 4.

B. Microcomputed Tomography

i. If you wish to proceed with microcomputed tomography, follow the protocol by Kallai et al. which describes methods for evaluation of bone regeneration via microcomputed tomography.[47] Alternatively, if you wish to evaluate angiogenesis and vasculature, proceed with the methods described by Patel et al., Young et al. and Duvall et al..[24,48,49]

Critical Step: MicroCT requires samples in a consistent environment throughout scanning, thus thawing or drying of samples during scanning can introduce artifact. Frozen samples should be thawed prior to scanning and wet samples should be wrapped in parafilm or other sealing medium prior to scanning.

Histological/Mechanical Analysis (Timing: Should take approximately 90 minutes for histology and 10 minutes for mechanical testing)

27 Perform histology (option 27A) or mechanical testing (option 27B).

A. Histology

i. To perform histology we recommend consulting the *Handbook of Histology Methods for Bone and Cartilage* by An and Martin for a complete discussion of methods.[50]

B. Mechanical Testing

i. Mount the push-out jig onto the mechanical testing system such that the specimen holder is in the stationary lower position with the 10 mm diameter hole concentrically aligned to the axis of the mechanical testing system.

ii. Mount the push-out rod to a 500 N load cell on the crosshead such that the 6 mm diameter rod is concentrically aligned to the 10 mm diameter hole.

Critical Step: The push-out jig described here allows for 2 mm clearance between the push-out rod and the hole below the specimen. Finite element analysis has previously shown this value must be above 0.7 mm to avoid peak stresses.[36]

iii. Remove the tissue specimen from the PBS, place on the tissue holder with the defect concentrically located over the hole with the cerebral surface facing upward and secure into place.

iv. Move crosshead as close to the specimen as possible without touching the specimen with the push-out rod.

v. Record the force and displacement as the crosshead moves into the specimen at 0.5 mm/min until after the peak force is reached.[23]

TIMING

Preoperative Preparation, steps 1–6: 20 minutes

Operative Procedure, steps 7–15: 30 minutes

Postoperative Care, steps 16 and 17: 90 minutes

Fluorochrome Labeling, steps 18–20: 5 minutes per injection

Euthanasia and Implant Harvest, steps 21–24: 30 minutes

Radiographic Analysis, step 25: 5 minutes for planar radiography and 2 hours for microcomputed tomography

Histological/Mechanical Analysis, step 26: 90 minutes for histology and 10 minutes for mechanical testing

TROUBLESHOOTING

Troubleshooting advice can be found in Table 1.

ANTICIPATED RESULTS

With the model described above, bone regeneration can be evaluated using a variety of techniques focusing on biological, structural and functional aspects of bone. Previously reported studies have utilized all of the described analytical methods and portions of those results are illustrated.

Surgical Procedure

Postoperatively, the rats recover quickly, returning to routine activities such as grooming, eating and drinking in less than 48 hr. With practice in the surgical procedure reducing dural tears, which may require exclusion from the study, the attrition can be reduced to less than 5%. Additionally, the attrition of animals has occurred in the first 48 hr allowing animal replacement and consistent sample sizes.

Mechanical Testing

In a study using either ceramic or polymeric scaffolds with bone marrow derived mononuclear cells and platelet rich plasma (PRP), the calvaria were tested mechanically after 12 weeks of implantation.[23] Figure 1 shows typical results from the peak loads, where the notation indicates the scaffold material, polymeric (P, Figure 1b) or ceramic (C, Figure 1c), the presence (P) or absence (-) of platelet rich plasma and the presence (M) or absence (-) of mononuclear cells. As expected, the mechanical performance is affected by the mechanical strength of materials placed into the defect, indicated by the increased peak load endured by the ceramic vs polymeric scaffolds.

Planar Radiography

As microcomputed tomography allows for more in-depth and quantitative analysis of bone formation within the defect, planar radiography has largely been replaced. However, in the absence of microCT, planar radiography can serve to give spatial information in regards to mineralization within the entire defect in a 2-dimensional manner. For example, in a study evaluating the release of plasmid DNA (pDNA) encoding the bone morphogenetic protein-2 (BMP-2) gene with a cytomegaloviral promoter from a hydrogel system, planar radiographs were taken of the removed specimens at 12 weeks. The study evaluated four groups: a material control of cationized gelatin microspheres (CGMS) in oligo(poly(ethylene glycol) fumarate) (OPF), a group of CGMS and OPF where 10 μg of pDNA was loaded into CGMS, a group of CGMS and OPF where 10 μg of pDNA was loaded into OPF and a group of CGMS and OPF where 100 μg of pDNA was loaded into OPF.[33] Representative planar radiographs from each group are shown in Figure 5. As can be seen in the representative planar radiographs, while a 2-dimensional image of mineralized tissue can be produced, other factors can affect the quality of the images such as soft tissue and lack of volumetric data. These data can be obtained through microcomputed tomography, but in the absence of the necessary equipment planar radiography can be applied to evaluate the defect area for mineralization.

Microcomputed Tomography

The protocol by Kallai et al. illustrates the evaluation of bone regeneration as measured by microCT with example results. The vascularity of the defect area can also be assessed through microCT. Another study from our laboratory investigated the dual release of angiogenic and osteogenic growth factors, vascular endothelial growth factor (VEGF) and bone morphogenetic protein-2 (BMP-2), respectively and typical results for microCT analysis can be found here.[24]

Histology

Several different stains can be applied to the histological sections of the defect. Additionally, both methylmethacrylate and paraffin embedding are possible if the materials introduced are soft enough and proper decalcification undertaken. However, our laboratory has generally performed methylmethacrylate embedding and sectioning. Figure 6 shows histological sections from the study comparing ceramic (A and B) and polymeric (C, D and E) scaffolds with bone marrow derived mononuclear cells (bmMNCs) and platelet rich plasma (PRP).[23] Various stains have been used and three are shown in Figure 6: Goldner's trichrome, hematoxylin and eosin and von Kossa/van Gieson. Goldner's trichrome staining is shown in A and D of a ceramic scaffold with PRP and a polymeric scaffold with PRP and bmMNCs, respectively. Goldner's trichrome is to show mineralized and non-mineralized osteoid seen in blue/green or red, respectively. The inset of Figure 6a shows mineralized and non-mineralized osteoid within the pores of the ceramic scaffold. The inset of Figure 6d shows the mineralized osteoid in the center of the polymeric scaffold. Hematoxylin and eosin staining is shown in B and E of a ceramic scaffold with PRP and bmMNCs and a polymeric scaffold alone, respectively. Hematoxylin and eosin is a general stain used to highlight cellular components, where the nuclei of cells are stained blue and the cytoplasm pink as seen in the inset of Figure 6e. Additionally, the stain colors fibrous tissue pink as in the inset of Figure 6b Finally, von Kossa/van Gieson staining is only shown for the polymeric scaffold (C) with bmMNCs, as the ceramic scaffold itself would stain positive. The von Kossa/van Gieson stain can be used to highlight mineralization of the scaffold by staining mineralized tissue black as seen in Figure 6c. High magnification insets for each section are shown to the right, where the scaffold material for both ceramic and polymeric implants is visible. While these staining techniques do not encompass all of the possible stains that could be used, these stains illustrate cellular and extracellular matrix components which can be visualized.

In addition to traditional histological sectioning and staining, fluorochrome labeling can be utilized to evaluate the temporal progression of mineral deposition. In a study using adenoviral, retroviral and cationic lipid gene therapy vectors delivering rhBMP-2 to harvested rat bone marrow stromal cells and then implanted into a calvarial defect with a titanium mesh, alizarin complexone and calcein were used to label the minerals deposited at 1 and 3 weeks, respectively.[31] Figure 7 shows merged fluorescent images of histological sections of the defect, which was implanted with adenoviral transfected rat marrow stromal cells on the titanium mesh. The large amounts of green fluorescence compared to red indicates the amount of mineral deposited was much greater at 3 weeks than at 1 week. Utilizing more than two fluorochromes can yield greater number of timepoints during the study without an increase in animals and gives temporospatial information on mineral deposition.

In conclusion, this model represents a rapid, reproducible critical size defect in the calvarium of the rat. Additionally, analytical techniques evaluating the regenerated tissue on the cellular, mineral and functional levels are illustrated. This model allows for consistent

evaluation of bone regeneration in a controlled *in vivo* environment in a cost-effective and rapid manner.

Acknowledgments

References

1. Giannoudis PV, Atkins R. Management of long-bone non-unions. Injury. 2007; 38:S1–2.

2. Giannoudis PV, et al. Nonunion of the femoral diaphysis. The influence of reaming and non-steroidal anti-inflammatory drugs. J Bone Joint Surg Br. 2000; 82:655–658. [PubMed: 10963160]

3. Schmitz JP, Hollinger JO. The critical size defect as an experimental model for craniomandibulofacial nonunions. Clin Orthop Relat Res. 1986; 205:299–308. [PubMed: 3084153]

4. Cancedda R, Giannoni P, Mastrogiacomo M. A tissue engineering approach to bone repair in large animal models and in clinical practice. Biomater. 2007; 28:4240–4250.

5. Reichert JC, et al. Establishment of a preclinical ovine model for tibial segmental bone defect repair by applying bone tissue engineering strategies. Tissue Eng Part B Rev. 2010; 16:93–104. [PubMed: 19795978]

6. Bodde EWH, Spauwen PHM, Mikos AG, Jansen JA. Closing capacity of segmental radius defects in rabbits. J Biomed Mater Res A. 2008; 85:206–217. [PubMed: 17688264]

7. Pearce AI, Richards RG, Milz S, Schneider E, Pearce SG. Animal models for implant biomaterial research in bone: a review. Eur Cells Mater. 2007; 13:1–10.

8. Einhorn TA. Clinically applied models of bone regeneration in tissue engineering research. Clin Orthop Relat Res. 1999:S59–67. [PubMed: 10546636]

9. Einhorn T, Lane J, Burstein A, Kopman C, Vigorita V. The healing of segmental bone defects induced by demineralized bone matrix. A radiographic and biomechanical study. J Bone Joint Surg Am. 1984; 66:274–279. [PubMed: 6693455]

10. Wang JC, et al. Effect of Regional Gene Therapy with Bone Morphogenetic Protein-2-Producing Bone Marrow Cells on Spinal Fusion in Rats. J Bone Joint Surg Am. 2003; 85:905–911. [PubMed: 12728043]

11. Henslee AM, et al. Biodegradable composite scaffolds incorporating an intramedullary rod and delivering bone morphogenetic protein-2 for stabilization and bone regeneration in segmental long bone defects. Acta Biomater. 2011; 7:3627–3637. [PubMed: 21757034]

12. Kempen DHR, et al. Retention of in vitro and in vivo BMP-2 bioactivities in sustained delivery vehicles for bone tissue engineering. Biomater. 2008; 29:3245–3252.

13. Kempen DHR, et al. Effect of local sequential VEGF and BMP-2 delivery on ectopic and orthotopic bone regeneration. Biomater. 2009; 30:2816–2825.

14. Kempen DHR, et al. Non-invasive monitoring of BMP-2 retention and bone formation in composites for bone tissue engineering using SPECT/CT and scintillation probes. J Control Release. 2009; 134:169–176. [PubMed: 19105972]

15. Freeman E, Turnbull RS. The value of osseous coagulum as a graft material. J Periodont Res. 1973; 8:229–236. [PubMed: 4269589]

16. Takagi K, Urist MR. The reaction of the dura to bone morphogenetic protein (BMP) in repair of skull defects. Ann Surg. 1982; 196:100–109. [PubMed: 7092346]

17. Ferland CE, Laverty S, Beaudry F, Vachon P. Gait analysis and pain response of two rodent models of osteoarthritis. Pharmacology, biochemistry, and behavior. 2011; 97:603–610.

18. Kim KS, et al. Small intestine submucosa sponge for in vivo support of tissue-engineered bone formation in the presence of rat bone marrow stem cells. Biomater. 2010; 31:1104–1113.

19. Muschler GF, Raut VP, Patterson TE, Wenke JC, Hollinger JO. The design and use of animal models for translational research in bone tissue engineering and regenerative medicine. Tissue Eng Part B Rev. 2010; 16:123–145. [PubMed: 19891542]

20. Hobar PC, Masson JA, Wilson R, Zerwekh J. The importance of the dura in craniofacial surgery. Plast Reconstr Surg. 1996; 98:217–225. [PubMed: 8764709]

21. Hobar PC, Schreiber JS, McCarthy JG, Thomas PA. The role of the dura in cranial bone regeneration in the immature animal. Plast Reconstr Surg. 1993; 92:405–410. [PubMed: 8341738]

22. Cooper GM, et al. Testing the critical size in calvarial bone defects: revisiting the concept of a critical-size defect. Plast Reconstr Surg. 2010; 125:1685–1692. [PubMed: 20517092]

23. Kretlow JD, et al. Uncultured marrow mononuclear cells delivered within fibrin glue hydrogels to porous scaffolds enhance bone regeneration within critical size rat cranial defects. Tissue Eng Part A. 2010; 16:3555–3568. [PubMed: 20715884]

24. Patel ZS, et al. Dual delivery of an angiogenic and an osteogenic growth factor for bone regeneration in a critical size defect model. Bone. 2008; 43:931–940. [PubMed: 18675385]

25. Bodde EWH, et al. The kinetic and biological activity of different loaded rhBMP-2 calcium phosphate cement implants in rats. J Biomed Mater Res A. 2008; 87:780–791. [PubMed: 18200544]

26. Ruhé PQ, et al. Biocompatibility and degradation of poly(DL-lactic-co-glycolic acid)/calcium phosphate cement composites. J Biomed Mater Res. 2005; 74:533–544.

27. Cooper GM, et al. Inkjet-based biopatterning of bone morphogenetic protein-2 to spatially control calvarial bone formation. Tissue Eng Part A. 2010; 16:1749–1759. [PubMed: 20028232]

28. Chesmel KD, Branger J, Wertheim H, Scarborough N. Healing response to various forms of human demineralized bone matrix in athymic rat cranial defects. J Oral Maxillofac Surg. 1998; 56:857–863. discussion 864–855. [PubMed: 9663577]

29. Schmökel HG, et al. Bone healing in the rat and dog with nonglycosylated BMP-2 demonstrating low solubility in fibrin matrices. J Orthop Res. 2004; 22:376–381. [PubMed: 15013099]

30. Schmökel HG, et al. Bone repair with a form of BMP-2 engineered for incorporation into fibrin cell ingrowth matrices. Biotechnol Bioeng. 2005; 89:253–262. [PubMed: 15619323]

31. Blum J, Barry M, Mikos AG, Jansen JA. In vivo evaluation of gene therapy vectors in ex vivo-derived marrow stromal cells for bone regeneration in a rat critical-size calvarial defect model. Hum Gene Ther. 2003; 14:1689–1701. [PubMed: 14670121]

32. Chew SA, et al. Delivery of plasmid DNA encoding bone morphogenetic protein-2 with a biodegradable branched polycationic polymer in a critical-size rat cranial defect model. Tissue Eng Part A. 2011; 17:751–763. [PubMed: 20964581]

33. Kasper FK, et al. Evaluation of bone regeneration by DNA release from composites of oligo(poly(ethylene glycol) fumarate) and cationized gelatin microspheres in a critical-sized calvarial defect. J Biomed Mater Res B Appl Biomater. 2006; 78:335–342.

34. Huang YC, Simmons C, Kaigler D, Rice KG, Mooney DJ. Bone regeneration in a rat cranial defect with delivery of PEI-condensed plasmid DNA encoding for bone morphogenetic protein-4 (BMP-4). Gene Therapy. 2005; 12:418–426. [PubMed: 15647766]

35. Kim SS, Kim BS. Comparison of osteogenic potential between apatite-coated poly(lactide-co-glycolide)/hydroxyapatite particulates and Bio-Oss. Dental materials journal. 2008; 27:368–375. [PubMed: 18717164]

36. Dhert WJ, et al. A finite element analysis of the push-out test: influence of test conditions. J Biomed Mater Res B Appl Biomater. 1992; 26:119–130.

37. Knothe UR, Dolejs S, Miller RM, Knothe Tate ML. Effects of mechanical loading patterns, bone graft, and proximity to periosteum on bone defect healing. J Biomech. 2010; 43:2728–2737. [PubMed: 20673900]

38. Krause WR, Bradbury DW, Kelly JE, Lunceford EM. Temperature elevations in orthopaedic cutting operations. J Biomech. 1982; 15:267–275. [PubMed: 7096382]

39. Mabbutt LW, Kokich VG, Moffett BC, Loeser JD. Subtotal neonatal calvariectomy. A radiographic and histological evaluation of calvarial and sutural redevelopment in rabbits. J Neurosurg. 1979; 51:691–696. [PubMed: 501409]

40. Persson KM, Roy WA, Persing JA, Rodeheaver GT, Winn HR. Craniofacial growth following experimental craniosynostosis and craniectomy in rabbits. J Neurosurg. 1979; 50:187–197. [PubMed: 430131]

41. Reid CA, McCarthy JG, Kolber AB. A study of regeneration in parietal bone defects in rabbits. Plast Reconstr Surg. 1981; 67:591–596. [PubMed: 7232579]

42. Mountziaris PM, Mikos AG. Modulation of the inflammatory response for enhanced bone tissue regeneration. Tissue Eng Part B Rev. 2008; 14:179–186. [PubMed: 18544015]

43. Mountziaris PM, Spicer PP, Kasper FK, Mikos AG. Harnessing and modulating inflammation in strategies for bone regeneration. Tissue Eng Part B Rev. 2011; 17:393–402. [PubMed: 21615330]

44. AVMA guidelines on euthanasia. American Veterinary Medical Association; 2007.

45. Research, I.o.L.A., Sciences, C.o.L. & Council, N.R. Guide for the Care and Use of Laboratory Animals. The National Academies Press; Washington D.C., USA: 1996.

46. Pelker RR, Friedlaender GE, Markham TC, Panjabi MM, Moen CJ. Effects of freezing and freeze-drying on the biomechanical properties of rat bone. J Orthop Res. 1983; 1:405–411. [PubMed: 6387075]

47. Kallai I, et al. Microcomputed tomography–based structural analysis of various bone tissue regeneration models. Nat Prot. 2011; 6:105–110.

48. Young S, et al. Dose effect of dual delivery of vascular endothelial growth factor and bone morphogenetic protein-2 on bone regeneration in a rat critical-size defect model. Tissue Eng Part A. 2009; 15:2347–2362. [PubMed: 19249918]

49. Duvall CL, Taylor WR, Weiss D, Guldberg RE. Quantitative microcomputed tomography analysis of collateral vessel development after ischemic injury. Am J Physiol Heart Circ Physiol. 2004; 287:H302–310. [PubMed: 15016633]

50. An, YH.; Martin, KL. Handbook of histology methods for bone and cartilage. Humana Press; Totowa, New Jersey, USA: 2003.
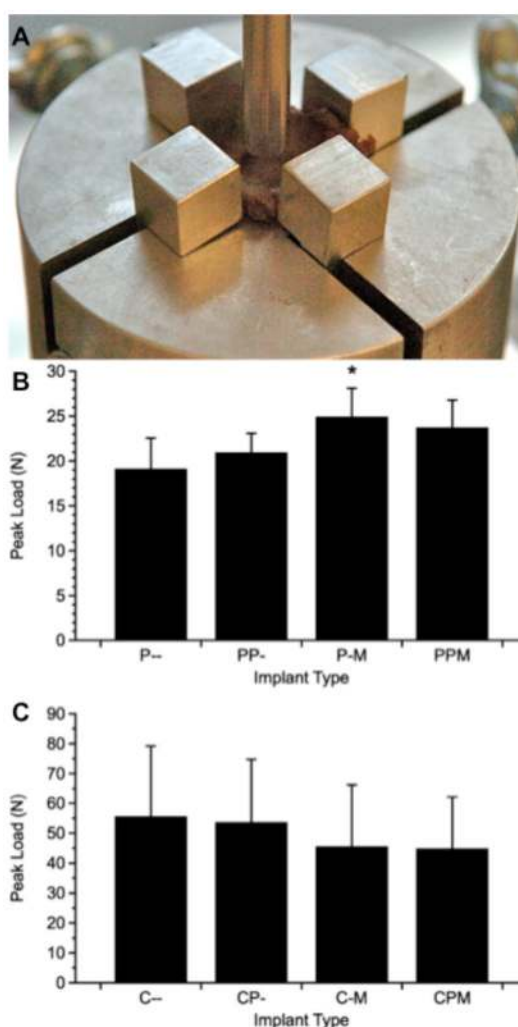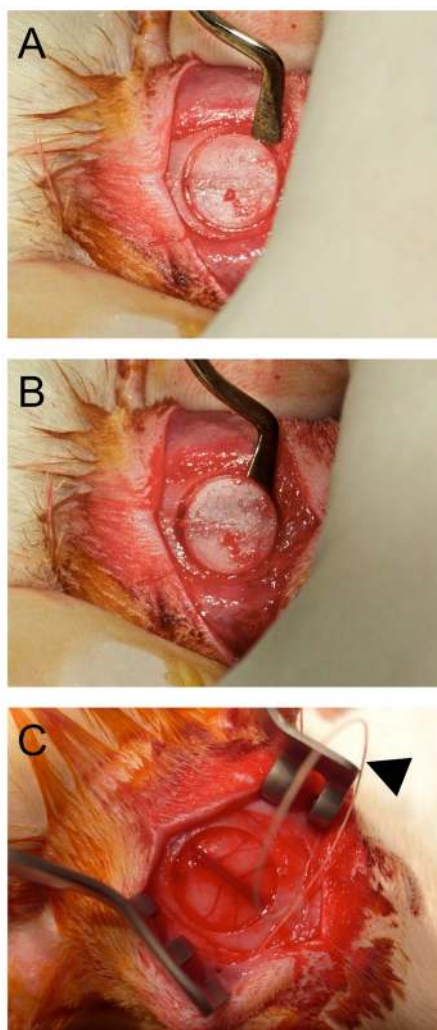
Figure 1.
Use of the push-out jig. (A) Photograph of push-out jig. The peak push-out load of the specimens (n = 6) with implanted (B) polymeric and (C) ceramic scaffolds with or without platelet rich plasma and/or bone marrow derived mononuclear cells. Implant type abbreviations denote the scaffold material (polymer, P or ceramic, C) followed by the presence or absence of platelet rich plasma (- or P, respectively) and the presence or absence of mononuclear cells (or M, respectively). * indicates significant difference from material control (p <0.05). Adapted with permission.[23]
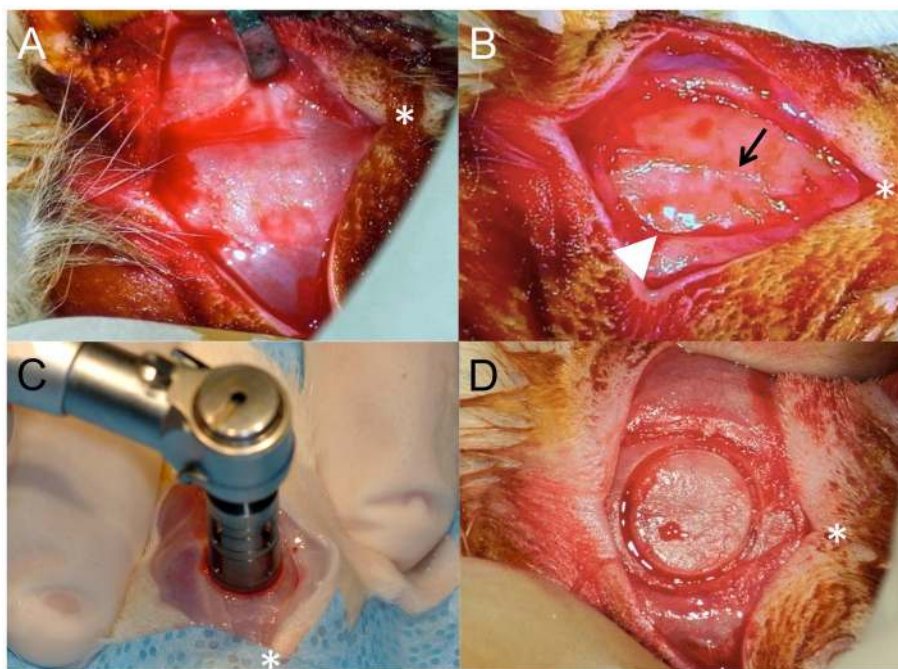
Figure 2.
Creation of the defect. The bone is exposed and the defect created by incision and retraction of the (A) skin and (B) periosteum (shown with white arrowheads) overlying the calvarium. Note the clear line of the sagittal suture in the bone of the calvarium indicated with a black arrow. A trephine with 8 mm diameter is used to cut the calvarial bone (C) resulting in a scored calvarium (D). * indicates the anterior side of the cranium.

Figure 3.
Use of the elevator. The elevator is used to gently lift the bone from the dura, first by (A) lifting the edge then (B) running the elevator under the surface to free any adherent dura. The exposed dura and brain beneath the defect are shown in (C). Additionally, a 4-0 Monocryl suture is seen loosely threaded through the periosteum indicated by the black arrowhead in (C). This technique of beginning the suture before trephination allows for easy apposition of the periosteal layer as it is very thin and delicate.

| Description	Score
Bony bridging entire span of defect at longest point (8 mm)	4
Bony bridging over partial length of defect	3
Bony bridging only at defect borders	2
Few bony spicules dispersed through defect	1
No bone formation within defect	0

Figure 4.
Scoring guide for extent of bony bridging and union. The gray areas in the circles represent mineralized tissue formed within the defect, which can be used for planar radiographs or microCT datasets. Reprinted with permission.[24]
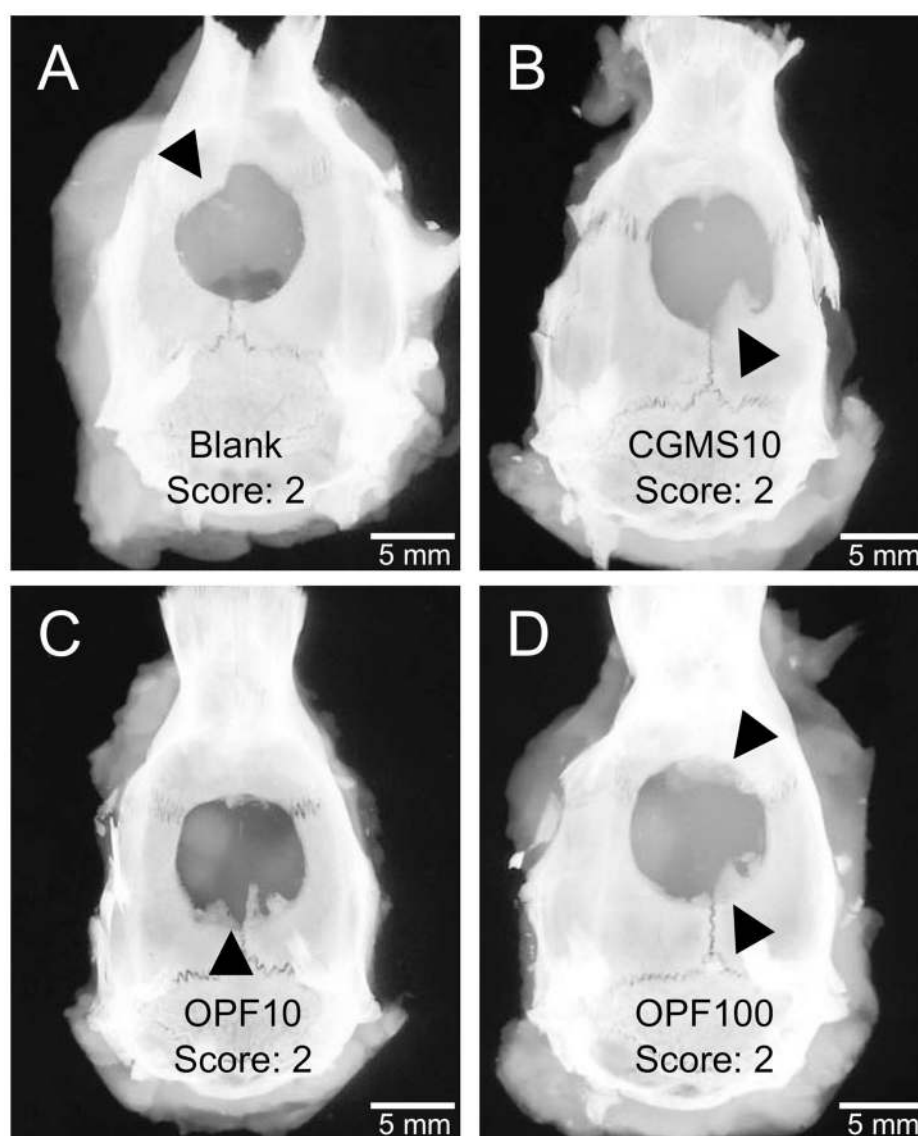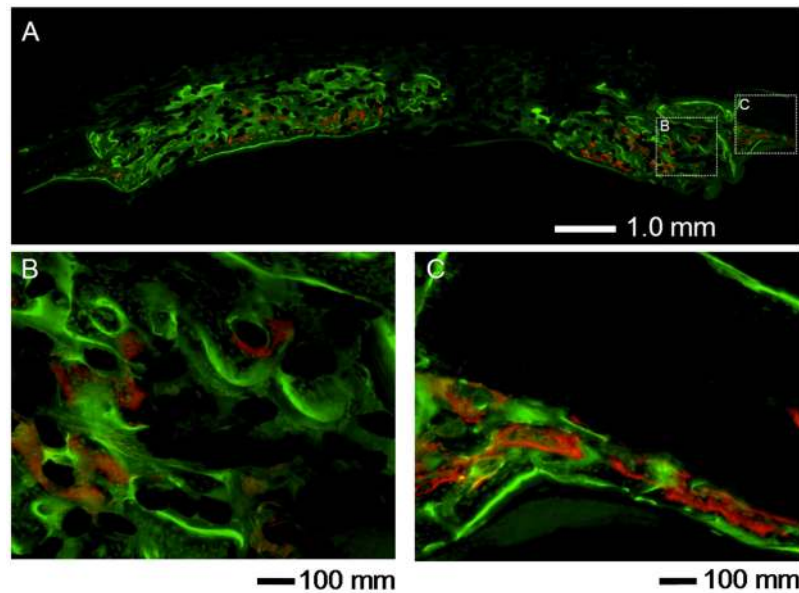
Figure 5.
Representative planar radiographs of defects at 12 weeks from a study looking at release of plasmid DNA encoding BMP-2 from a hydrogel (OPF) with gelatin microparticles (CGMS). The images show specimens implanted with (A) OPF and CGMS, (B) OPF and 10 µg of pDNA in the CGMS phase, (C) CGMS and 10 µg of pDNA in the OPF phase and (D) CGMS and 100 µg of pDNA in OPF phase.[33] Arrowheads indicate the areas of bone growth into the defect.
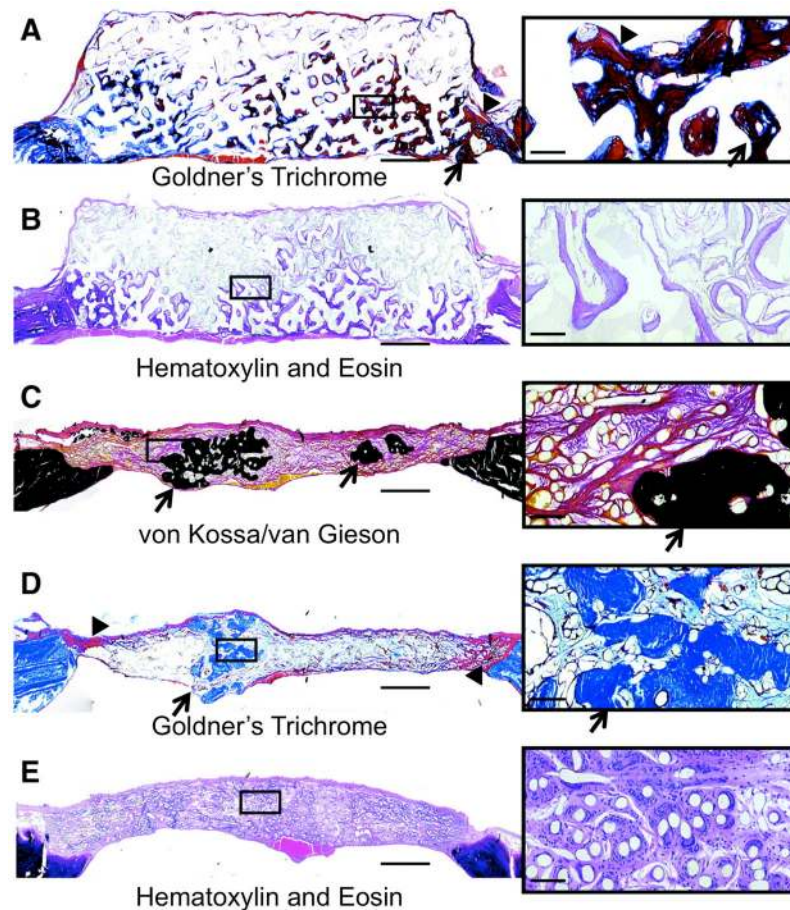
Figure 6.
Histological sections cut coronally through the defect after 12 weeks of implantation.
Ceramic (A–B) and polymeric (C–E) scaffolds were used in combination with platelet rich
plasma (PRP) and/or bone marrow derived mononuclear cells (bmMNCs). The sections are
stained with (A, D) Goldner's trichrome, (B, E) hematoxylin and eosin and (C) von Kossa/
van Gieson and show representative sections from the (A) ceramic scaffold with PRP group,
(B) the ceramic scaffold with PRP and bmMNCs, (C) the polymeric scaffold with bmMNCs,
(D) the polymeric scaffold with PRP and bmMNCs and (E) the polymeric scaffold alone.
Arrows indicate mineralized tissue and arrowheads indicate non-mineralized osteoid. Scale
bars for the full size images on the left represent 1 mm, while scale bars for the higher
magnifications on the right represent 100 µm. Adapted with permission.[23]

Figure 7.
Fluorescent image of a coronally oriented histological section showing temporal fluorochrome labeled mineral deposition. This study implanted titanium meshes seeded with bone marrow derived marrow stromal cells transfected with an adenoviral vector of BMP-2. Red fluorescence is due to alizarin complexone injected at 1 week and green fluorescence is due to calcein injected at 3 weeks postoperatively. Insets (B) and (C) show high magnification (10X) images of the section indicated by the white boxes in the image of the full defect (A) at low magnification (2.5X). Reprinted with permission.[31]

Table 1

Troubleshooting

Step	Problem	Possible Reason	Solution
5	The heart rate increases.	The depth of anesthesia is too low and the animal is experiencing pain.	Increase the percentage of isoflurane in the flow of oxygen to increase anesthetic depth.
5	The saturation of hemoglobin falls.	The depth of anesthesia is too high and the animal is experiencing respiratory depression.	Decrease the percentage of isoflurane in the flow of oxygen to decrease anesthetic depth. A clear plastic drape is preferred because respirations, movement and coloring of the animal can be monitored throughout the procedure.
7	The trephine snags soft tissue during creation of the defect.	The exposure of bone and retraction of skin, soft tissue and periosteum is insufficient.	Elevate more periosteum to create a larger surgical field. Also, a longer incision can increase the spread of the skin and soft tissues. Additionally, an assistant may be needed to aid in soft tissue retraction.
9	The trephine has completely cut through one section of bone (typically the anterior and posterior sections of the defect border) but other sections of bone are too thick for the circular bone segment to be raised from the underlying dura.	The curvature of the skull prevents straight cutting with a trephine to produce even cutting through all segments of the calvarium.	Precess the trephine about the axis perpendicular to the calvarium to evenly cut the bone.
11	The dural tissue adheres to the bone and produces a tear with or without hemorrhage of the sagittal sinus.	The dural tissue is not adequately freed from the cerebral side of the calvarium.	In addition to slow careful blunt dissection using a thin elevator, saline soaked gauze may be passed gently back and forth between the dura and cerebral side of the calvarium to bluntly and gently separate the tissues.
11	There is profuse bleeding in the defect.	The sagittal sinus has been torn.	Rinse with normal saline and apply gentle pressure. Due to concerns of variability this animal should be considered for removal from the study.
16	The incision wound does not heal properly resulting in excessive swelling or redness.	The skin incision may have become infected.	Prophylactic antibiotic ointment placed on the incision immediately after closure may aid in wound healing.
17	The animal does not recover as expected as observed by unresolved porphyrin staining, weight loss, decreased grooming or altered neurological activity such as seizures or gait abnormalities.	There is likely an unforeseen process due to the surgery, implant or manipulation such as excess inflammation, swelling or blood loss, infection, or implant failure.	Daily weights should be documented to monitor progress. Treats and intraperitoneal injections of normal saline should be used in cases of greater than 10% weight loss.
24	The explanted sample breaks upon excision or manipulation.	A sufficient amount of bone was not harvested during excision.	A larger amount of bone surrounding the implant should be harvested during excision.
26	The planar radiographs do not show enough contrast, such as to differentiate thin bone segments from soft tissue or thick bone from thin bone segments.	The exposure settings for the x-ray machine have not been optimized for the film, screen and x-ray system.	Changes in exposure time, tube voltage, tube amperage, film and screen can be used to alter image contrast.